DOI: 10.1007/s12541-012-0128-x

Human-Robot Cooperative Control Based on pHRI (Physical Human-Robot Interaction) of Exoskeleton Robot for a Human Upper Extremity

Heedon Lee[1], Byeongkyu Lee[1], Wansoo Kim[1], Myeongsoo Gil[2], Jungsoo Han[3], and Changsoo Han[1,#]

1 Dept. of Mechanical Engineering, Hanyang University, 1271, Sa-dong, Sangrok-gu, Ansan-si, Gyeonggi-do, Republic of Korea, 426-791
2 Dept. of Mechatronics Engineering, Hanyang University, 1271, Sa-dong, Sangrok-gu, Ansan-si, Gyeonggi-do, Republic of Korea, 426-791
3 Dept. of Mechanical System Engineering, Hansung University, 389, Samseon-dong 2-ga, Seongbuk-gu, Seoul, Republic of Korea, 136-792
Corresponding Author / E-mail: cshan@hanyang.ac.kr, TEL: +82-31-400-5247, FAX: +82-31-406-6398

KEYWORDS: Human-robot cooperation control, Physical human-robot interaction, Wearable robot, Exoskeleton, Power assistive robot

This paper proposes a human-robot cooperative control of exoskeleton robot assisting muscle strength of a human upper extremity when lifting or transporting heavy objects. When a human wears a robot, the motions of the human and robot generate interaction, which is called HRI (Human-Robot Interaction). To generate reference motion from the interaction force, a pHRI model was developed using virtual mechanical impedance, and an experimental method to determine the impedance parameters of the pHRI model was proposed. The controller was developed in such a way that the desired motion will be controlled using dynamic model-based compensation. To verify the proposed control method, it was applied to an exoskeleton robot with 6-DOF for both arms. Motion-following-performance experiment and muscle-strength-assisting-effect experiment were conducted using this robot. Experimental results, the wearer of the exoskeleton robot can handle a small force was the heavy object.

Manuscript received: November 23, 2011 / Accepted: January 31, 2012

NOMENCLATURE

F_{HR} = human-robot interaction force
ω_n^{HR} = natural frequency of the pHRI model
ω_n^H = natural frequency of a human arm
ζ^{HR} = damping ratio of the pHRI model
ζ^H = damping ratio of a human arm
M_p^H = % overshoot of a human arm
t_r^H = rising time of a human arm

1. Introduction

Generally, robots are operated by programmed logics, by sensing information, and with artificial intelligence. These robots must be programmed with algorithm for the expected environment or be installed with artificial intelligence for the appropriate situation. This control strategy, however, has limits on robot use and performance. Recently, many researchers have attempted to develop a human force augmentation system, namely an exoskeleton robot system, to allow humans to physically utilize the robot-generated force. An exoskeleton robot system is force-assistive in a variety of environments. In this system, humans manipulate posture control of the robot, situation awareness, and generation of operating signal. The exoskeleton robot for force-assisting imitates the joints of the human. This area of study is expected to contribute to the industry for senior citizens, the medical service, and military equipment for soldiers in an effort to reduce and/or eliminate the burden on the user's back. The benefits are also applicable in industrial settings, among others, in which heavy material handling workers work.

Exoskeleton robots have been studied at U.C. Berkeley since the 1980s, and other countries have been researching exoskeleton robots since the 20th century. Kazuo Kiguchi (2001) developed an upper extremities power-assistive robot, possessing 3 DOF (degrees of freedom), for the old and handicapped, using the Fuzzy-Neuro control.[1] Takashi Matsuo (2002) suggested the HARO for power assistance for nurses, enabling them to lift and transfer patients.[2] Younkoo Jeong (2000) suggested an upper extremity assistive system where parallel robots[3] are attached to the human body. Tetsuya Morizono (1999) developed a power assistive system using artificial muscle and a pneumatic cylinder in a spacesuit.[4] Jacob

Rosen (2007) suggested an upper limb powered exoskeleton system based on a muscle model using the EMG (electromyogram) signals.[5] Masaaki Kobayashi (2009) developed an upper limb power assist system using pneumatic actuators for farming lift-up motion.[6] Haifa Mehdi suggested a position/force cooperative control method for rehabilitation of a human arm supported by a robotic manipulator.[7] Tsukasa Ogasawara (2008) suggested a pinpointed muscle force control for power assisting device.[8] E. Sanchez (2007) suggested an optimal control method using the LQG (Linear Quadratic Regulator) for human power enhancement.[9] H. Kazerooni (1990) suggested an upper extremities system for assisting the delivery of a missile.[10] He (H. Kazerooni 2006) also developed a wearable lower extremities assistance robot for infantry, called the BLEEX (Berkeley Lower Extremity Exoskeleton).[11] Yoshiyuki Sankai (1993) developed the HAL (Hybrid Assistive Leg), which is an assistive lower extremity for the old, the weak, and the disabled.[12] Xiaopeng Liu (2005) proposed an assistive system for the lower extremities, developed for transferring heavy burdens.[13] Force assistive exoskeleton robots used for force-assisting differ depending on assistive region and sensor type. The assistive regions are those that make up the upper limbs, leg, and integration systems. And, the sensor type is formed by an EMG sensor, force sensor, and hybrid types.[14]

In this paper, we suggest a human-robot cooperative control for the force assistive exoskeleton robot based on physical human-robot interaction. We developed force assistive exoskeleton robots for the upper extremities with the proposed control method. To verify the proposed control method, a motion following performance experiment and a muscle strength assisting effect experiment were conducted using an exoskeleton robot with 6-DOF for both arms. The exoskeleton robot used in these experiments was developed to have a structure that is appropriate for the target task, and can perform shoulder E/F (extension/flexion), shoulder Ab/Ad (abduction/adduction) and elbow E/F motions. Furthermore, to measure interaction force, 3-axes force sensor is used at the interaction points between human and robot.

2. pHRI (physical human-robot interaction) Modeling

2.1 Background

For human-robot cooperative control of an exoskeleton robot, we need to understand the command signal system for motions of the robot and the forces generated by the motions. When a human is combined with a robot, the motions of the human and robot generate interaction, and this is called HRI (human-robot interaction).

Fig. 1 shows the HRI generated when a human is wearing a robot. HRI can be divided into cHRI (cognitive human-robot interaction) and pHRI (physical human-robot inter-action).[15,16] cHRI is the interaction related to bi-directional cognitions (inference, planning, and action) between human and robot, whereas pHRI is the interaction related to the forces generated between the musculoskeletal system and the rigid body of the robot. This type of HRI can be measured and be used as an input to the robot controller. In this study, pHRI was measured using force sensors and used as an input to the robot controller. The wearer performs the target tasks when the change of force between the human and robot is fed back by the robot to the central CNS (central nervous system) or the brain through the sense organs of the wearer.

2.2 pHRI Model using the Mechanical Impedance

pHRI is the interaction of forces between human and robot. The desired motion of the user must be understood from the measured forces and the command signals for the robot must be generated accordingly. The exoskeleton robot used in this study is attached to the back of a human user through the robot base, and interaction forces are generated only by the connected wrist interface. Fig. 2 illustrates this. As shown in this figure, pHRI is modeled using the virtual impedance parameters of the wrist interface M_{HR}, B_{HR} and K_{HR} to give mechanical characteristics.

This model shows the relationship between the interaction force and the position, speed and acceleration desired by the wearer. Eq. (1) is the dynamic equation of the pHRI model.

$$F_{HR} = M_{HR}\ddot{p}_d + B_{HR}\dot{p}_d + K_{HR}p_d \quad (1)$$

Here, F_{HR} is the interaction force between human and robot,

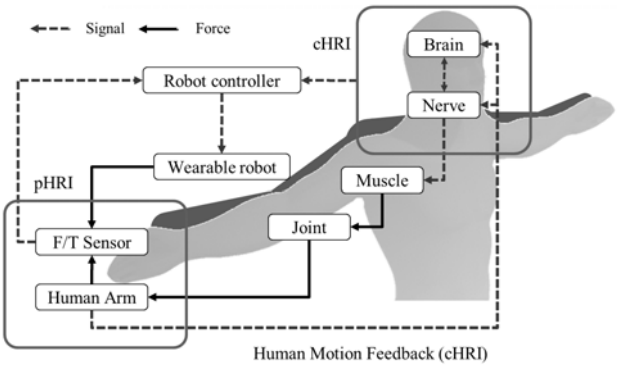

Fig. 1 Physical and cognitive human-robot interaction

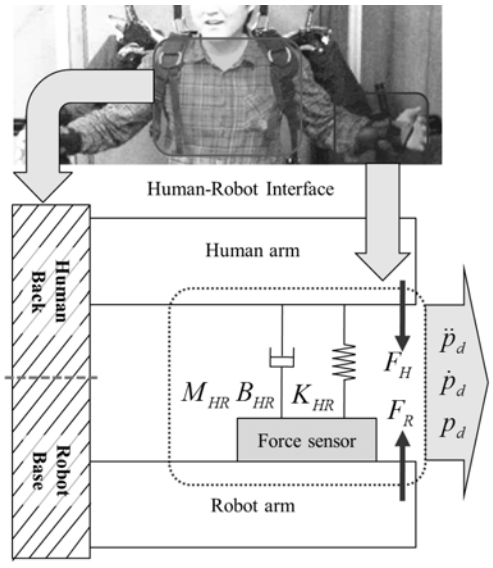

Fig. 2 pHRI Model using the virtual mechanical impedance

which is measured by the 3-axes force sensor mounted on the wrist interface.

Among the impedance parameters, K_{HR} is related to the desired position of the wearer against the inputted interaction force, and is directly controlled by the wearer. M_{HR} and B_{HR} are determined by an experimental method considering control responsiveness and stability.

2.3 Adjustment of Impedance Parameters

To determine M_{HR} and B_{HR} among the impedance parameters of the pHRI model, ω_n^{HR} and ζ^{HR} were used. These parameters determine the responsiveness and stability of the pHRI model. ω_n^{HR} and ζ^{HR} for the pHRI model can be derived by eq. (3) from the transfer function of eq. (2).

$$H(s) = \frac{1}{M_{HR}s^2 + B_{HR}s + K_{HR}} \tag{2}$$

$$\omega_n^{HR} = \sqrt{\frac{K_{HR}}{M_{HR}}}, \quad \zeta^{HR} = \frac{B_{HR}}{2\sqrt{M_{HR}K_{HR}}} \tag{3}$$

Here, since K_{HR} is determined by the user, M_{HR} and B_{HR} can be calculated by eq. (4) once ω_n^{HR} and ζ^{HR} are determined.

$$M_{HR} = \frac{K_{HR}}{\left(\omega_n^{HR}\right)^2}, \quad B_{HR} = 2\zeta^{HR}\sqrt{M_{HR}K_{HR}} \tag{4}$$

Since the purpose of an exoskeleton robot is to follow the arm motion of a human, ω_n^{HR} and ζ^{HR} must be determined to provide responsiveness to the motion of a human arm. Thus, in this study, ω_n^{H} and ζ^{H} were calculated using eq. (5) with M_p^H and t_r^H which were measured through motion experiment of the human arm, and substituted with ω_n^{HR} and ζ^{HR} in eq. (4) to determine the M_{HR} and B_{HR} of the pHRI model which have similar motion characteristics as those of human arm.

$$\omega_n^H = \frac{\pi - \tan^{-1}\left(\dfrac{\sqrt{1-\left(\zeta^H\right)^2}}{\zeta^H}\right)}{t_r^H\sqrt{1-\left(\zeta^H\right)^2}}, \quad \zeta^H = \frac{\ln M_p^H}{\sqrt{\pi^2 + \left(\ln M_p^H\right)^2}} \tag{5}$$

The pHRI model was created using virtual impedance parameters, which are determined using the analysis results of the motion characteristics of a human arm. Fig. 3 illustrates the measurement method for human arm motions. As shown in this figure, the experiment on the human behavioral characteristics of the moving hand position was measured. At this point, the human arm is controlled with visual feedback. This experiment intends to find M_p^H and t_r^H by measuring and analyzing the motions of a human arm using the joint angle and forward kinematics measured with an encoder. However, since M_p^H and t_r^H are the response characteristics of the control system under the given step input, two assumptions are needed for this experiment. First, the intention of the user to move fast from the start point to the target point is identical to the step input for the position. Second, the human arm can perfectly position control through visual feedback.

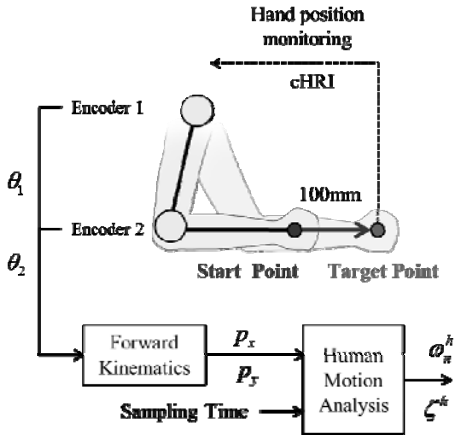

Fig. 3 Experimental system of the human arm motion analysis for impedance parameter adjustment

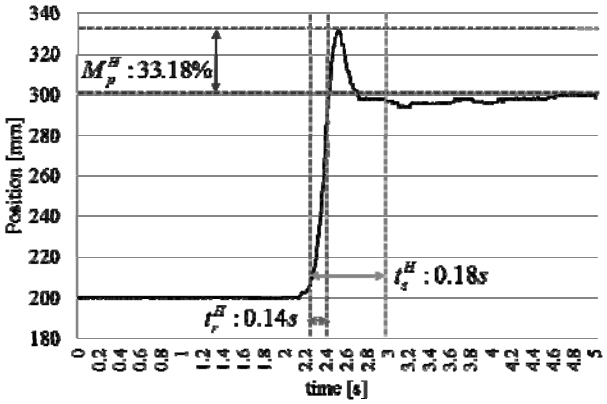

Fig. 4 Analysis result of the human hand position

Table 1 Comparison of measured roughness data

	K_{HR} [N/m]	M_{HR} [kg]	B_{HR} [N/m/s]
Case 1	100	0.062	6.378
Case 2	150	0.093	9.567
Case 3	200	0.123	12.756
Case 4	300	0.185	19.133

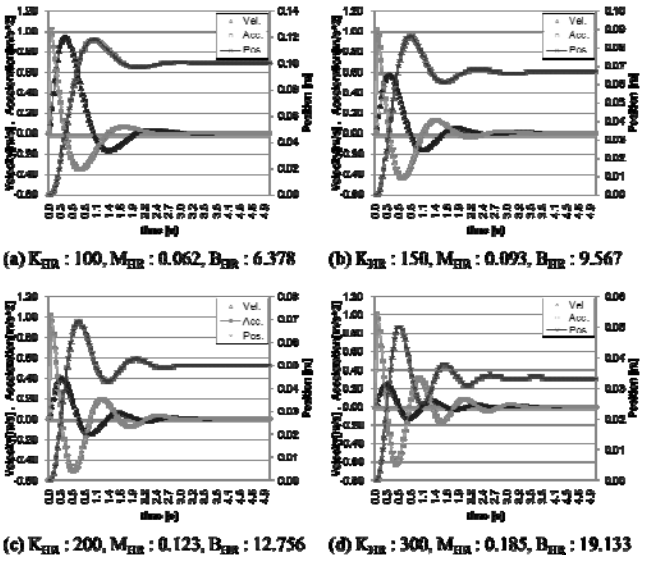

Fig. 5 Simulation result of unit-step response to pHRI model (input force 10N)

Fig. 4 shows the measurement results of the human arm motions. M_p^H is 33.18% and t_r^H is 0.14 sec. Thus, by eq. (5), ω_n^H is 12.86 Hz and ζ^H is 0.41. If K_{HR} is determined by the wearer, M_{HR} and B_{HR} of the pHRI model can be determined by eq. (4). To evaluate the responsiveness and stability of the pHRI model determined through this experiment, M_{HR} and B_{HR} were derived by K_{HR} for each of the four cases in Table 1, and the output position, velocity and acceleration were simulated when the step input of 10N was given.

Fig. 5 shows the simulation results for each case. The M_{HR} and B_{HR} determined in accordance with K_{HR} show that the outputs of pHRI model are all stable. Therefore, the wearer can generate stable robot control input by directly setting K_{HR} that is most appropriate for oneself.

3. Control Strategy

3.1 Control Strategy of Human-Robot Cooperation

For exoskeleton robots, the user directly controls much of the human-robot cooperative control such as task command generation, environmental perception, and feedback control of robot motions. Hence, the exoskeleton robot controller must understand the desired motion of the user and perform motion control based on this to follow the motion of the user. Fig. 6 shows the block diagram of the control system for human-robot cooperative control of an exoskeleton robot. As shown in this figure, the wearer can understand the given task, environment, and robot condition through sensory organs, and moves his/her arm using this information. Since the exoskeleton robot is attached to the user at the wrists as shown in Fig. 2, interaction force is generated between the user and the robot by the motion of the human arm, and the desired motion can be generated by pHRI modeling of this force. Therefore, the resulting desired motion contains the desired motion of the wearer, who controls the joints of the exoskeleton robot using the motion controller.

3.2 Motion Control of the Exoskeleton Robot

In the previous chapter, desired motion of an end-effector is generated using the pHRI model. In this section, the motion control problem for an exoskeleton robot can be formulated by finding the joint torques which ensure that the end-effector attains a desired position. A classical strategy to control this type of mechanical system is inverse dynamics control, which is aimed at linearizing and decoupling the robot dynamics via feedback. Nonlinearities such as coriolis and centrifugal torques, and gravity torques can be nearly cancelled by adding these terms to the control input, while decoupling can be achieved by weighting the control input by the inertia matrix. According to this dynamic model-based compensation, the joint torques can be derived using eq. (6)

$$\tau = M_R(q)\alpha + C_R(q,\dot{q})\dot{q} + G_R(q) \tag{6}$$

The goal is to design a position control action to ensure tracking of a desired end-effector position trajectory. Therefore, the new control input α can be derived as

$$\alpha = J^{-1}(q)\left(a - \dot{J}(q,\dot{q})\dot{q}\right) \tag{7}$$

Where a means the resolved acceleration in terms of end-effector variables.

$$\begin{aligned} &a = \ddot{p}_d + K_D\Delta\dot{p}_{dr} + K_P\Delta p_{dr} \\ &where,\ \ \Delta p_{dr} = p_d - p_r \end{aligned} \tag{8}$$

K_D and K_P are suitable feedback matrix gains. Therefore, the closed-loop dynamic behavior of the position error is eq. (9)

$$\Delta\ddot{p}_{dr} + K_D\Delta\dot{p}_{dr} + K_P\Delta p_{dr} = 0 \tag{9}$$

The system (eq. (9)) is exponentially stable for any choice of positive definite K_D and K_P, thus tracking of p_d and $\dot{p}_d$ is ensured.

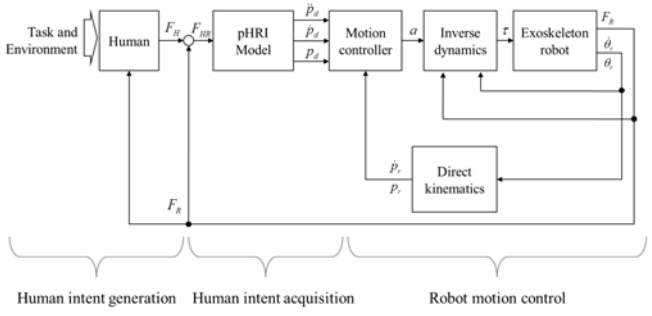

Fig. 6 Block diagram of the control system for human-robot cooperation work of an exoskeleton robot

4. Exoskeleton Robot System for Experiment

Among others, the shoulder joint has an axis of rotation at a single point; therefore in this experiment, we assumed the shoulder joint as a spherical joint. The exoskeleton robot is connected to the human body via the exoskeleton, and the exoskeleton robot's rotation centers of joints must be adapted to the rotation centers of the human body. Especially, the shoulder joints of the exoskeleton are difficult to adapt to the rotation centers of the human body because a human shoulder joint is spherical. Also, the command signal to control the robot is difficult to generate because the collective motion of the human arm has many DOF. Therefore, the design of the exoskeleton robot needs a task definition in order to operate.[17,18]

The exoskeleton robot used in this study has 3-DOF in the shoulder and 1-DOF in the elbow. A Fig. 7 depicts the work area and the assistive motion of a human. The actuators support shoulder E/F, shoulder Ab/Ad, and elbow E/F DOF. Moreover, the exoskeleton is manufactured to fit the general body size of males aged 20-29. The shoulder and elbow ROM (range of motion) of the proposed exoskeleton robot was based on standard Korean male data.[19] The exoskeleton robot used in this research is designed so that it can connect to the human-robot interface. In addition, the link length of this robot is able to adjust to the rotation center of the human joint and the exoskeleton joint so that the two may integrate.

Lack of integration may be caused by a difference in a person's physical dimensions or by the disagreement between the rotation centers of the human and robot joints.

This system has a shifted shoulder joint for horizontal Ab/Ad. This design is convenient, and more importantly, the joint is not actuated. As a result, the design of this system is simple and the interference among the three axes is more or less prevented. The proposed system has two points of contact: the back and the wrist of the user. The human-robot interface is important for the wear sensation and convenience of the device, which we considered when planning the orthotics.

This interface connects the human and robot, giving the user a natural feel, facilitating comfort and convenience, as shown in Fig. 8. This system was designed by considering the quality of the force sensor because of the attachment at the module. This system uses the command signal of the exoskeleton robot and the measured the relative force between the user and the exoskeleton robot from the 3-axes load-cell.

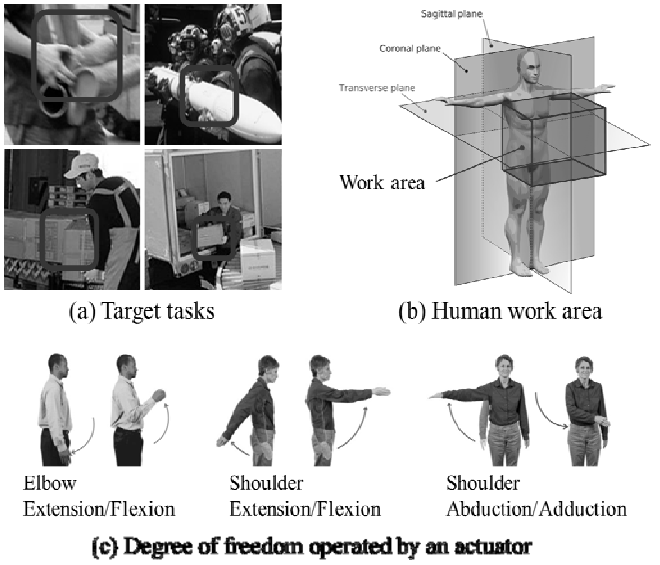

Fig. 7 Target tasks and the degree of freedom of the assistive exoskeleton robot

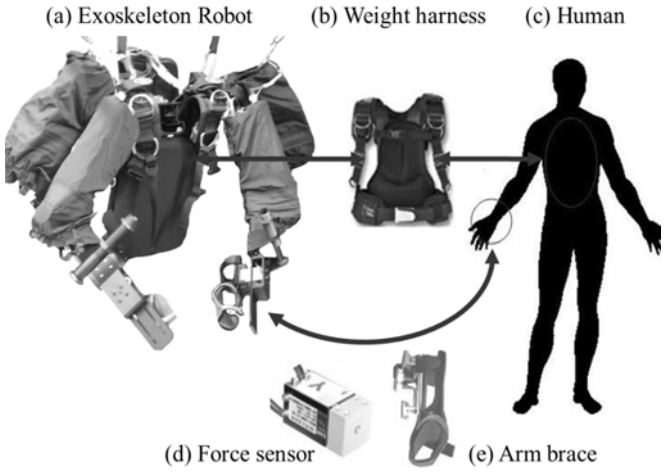

Fig. 8 Power assistive exoskeleton robot system for the human upper extremity

5. Experiment and Results

5.1 Muscle Strength Assisting Effect

Exoskeleton robots are used to assist the muscle force of users. Therefore, the effects of muscle force assistance need to be verified. For this purpose, this experiment measured and compared the muscle activity of the user with or without the robot using EMG sensors during elbow extension/flexion and shoulder extension/flexion motions. The weight of the handled object in this experiment was 10 kg. The EMG sensors were attached to biceps brachii, triceps brachii, deltoid posterior, and deltoid anterior. The signals were measured at 1024 Hz. During this experiment, the biceps brachii muscle is the muscle mainly responsible for flexion and the triceps brachii is the muscle mainly responsible for extension of the elbow joint. And, the deltoid posterior muscle is the agonist muscle for extension and the deltoid anterior muscle is the agonist muscle for flexion of the shoulder joint.

Fig. 9 shows the muscle activity measurements for elbow E/F

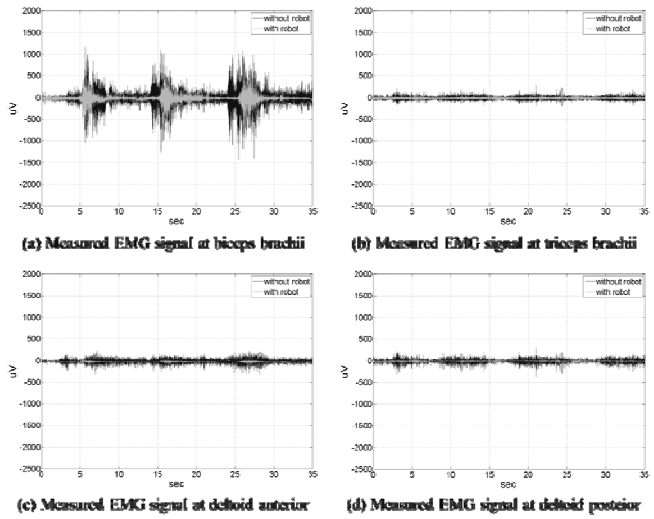

Fig. 9 Muscle activity measurements for elbow extension/flexion motion

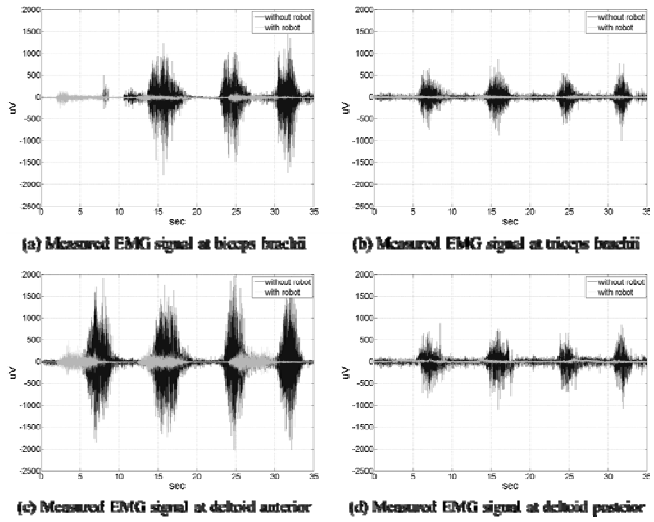

Fig. 10 Muscle activity measurements for shoulder extension/flexion motions

motions. As this figure shows, the muscle activity of the biceps decreased while triceps, deltoid posterior and deltoid anterior were hardly activated when the user used the exoskeleton robot. Fig. 10 shows the experiment results for shoulder E/F motions. All muscles except the deltoid posterior, which is an agonist, were activated when the user did not wear the robot. When user used the exoskeleton robot, however, the muscle activity of deltoid posterior decreased whereas biceps, triceps and deltoid anterior were hardly activated.

Fig. 11 shows the comparison of the required muscle activation when wearing the robot system and when not wearing it. Comparing these maximum values, the EMG signals with the exoskeleton robot is smaller then those without the exoskeleton robot. Therefore, the exoskeleton robot using the human-robot cooperative control developed in this study assisted the muscle strength of the wearer and was controlled as desired.

5.2 Motion Following Performance

This section describes the experiment on the following performance of the exoskeleton robot conforming to the motion of the wearer. For this experiment, the positions of the human arm and the robot's end-effector were measured and compared. To measure the position of the human arm, an electro-goniometer was attached to the human arm to measure the joint angle and the position was calculated using forward kinematics.

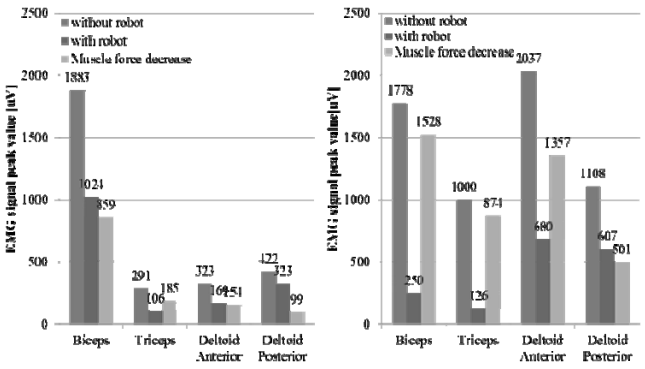

(a) Elbow extension/flexion (b) Shoulder extension/flexion

Fig. 11 Comparison of maximum values of EMG signals

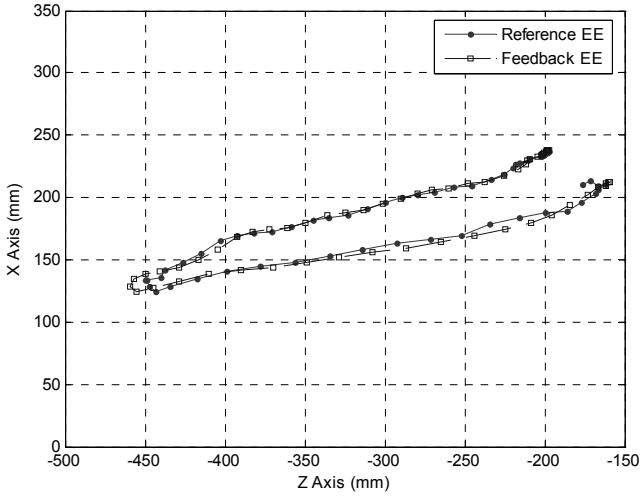

Fig. 12 End-effector position of human and exoskeleton robot

Fig. 12 shows the positions of the human arm and the robot's end-effector when $K_{HR} = 150$ N/m, $M_{HR} = 0.093$ kg, $B_{HR} = 9.567$ N/m/s for the impedance parameters of the pHRI model and $K_D = 10$ and $K_P = 500$ for the motion controller. Here, reference EE is the position of the user, and the feedback EE is the position of the exoskeleton robot's end-effector. This experiment proved that the exoskeleton robot using the human-robot cooperative control developed in this study followed the motions of the wearer.

As shown in Fig. 13, 6-DOF movement tests were carried out with a user wearing the exoskeleton robot applying the control method developed in this study. We have operated the elbow E/F, shoulder E/F, and shoulder Ab/Ad motions.

6. Conclusions

In this study, a human-robot cooperative control method was developed for an exoskeleton robot for the purpose of assisting the muscle force of human upper extremity. The proposed control method generated the desired motion of the exoskeleton robot using the interaction force generated by physical human-robot interaction, and the exoskeleton robot followed the desired motion. To generate reference motion from the interaction force, a pHRI model was developed using virtual mechanical impedance, and an experimental method to determine the impedance parameters of the pHRI model was proposed. To evaluate the responsiveness and stability of this pHRI model, a simulation was performed with the step input of 10N, and the results showed that the desired motion was stable. But virtual impedance parameters of pHRI must be experimentally adjusted to accommodate the user's wear sensation. Therefore, a calibration algorithm needs to be studied to adjust the parameters according to the wearer's comfortability.

The controller of the exoskeleton robot for human-robot cooperation uses the generated desired motion as input, and was

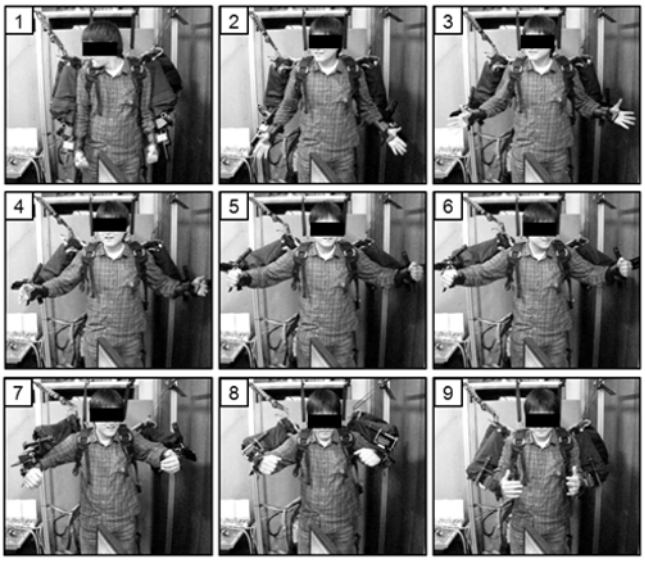

Fig. 13 6-DOF movement test of the exoskeleton robot by the human-robot cooperative control

designed to enable motion control using dynamic model-based compensation. To verify the proposed control method, it was applied to an exoskeleton robot with 6-DOF for both arms. Motion-following-performance experiment and muscle-strength-assisting-effect experiment were conducted using this robot. For motion following performance experiment of the exoskeleton robot, the motions of the wearer and the exoskeleton robot were measured and compared. As a result, the exoskeleton robot was found to follow the wearer's arm motions. Furthermore, during muscle-strength-assisting-effect experiment, we measured the muscle activity of the wearer using EMG signals while the user was handling a 10 kg object. It was found that the muscle activity decreased when the wearer used the exoskeleton robot. This implies that the user can handle a heavy object with a smaller force when the user wears the exoskeleton robot. Therefore, we can conclude that the pHRI-based human-robot cooperative control proposed in this study is appropriate for exoskeleton robots for handling heavy objects with human upper extremities.

ACKNOWLEDGEMENT

This research was supported by the Happy tech. program through the National Research Foundation of Korea (NRF) funded by the Ministry of Education, Science and Technology (No. 2011-0020938).

REFERENCES

1. Kiguchi, K., Rahman, M. H., Sasaki, M., and Teramoto, K., "Development of a 3DOF mobile exoskeleton robot for human upper-limb motion assist," Robotics and Autonomous Systems, Vol. 56, No. 8, pp. 678-691, 2008.
2. Yamamoto, K., Hyodo, K., Ishii, M., and Matsuo, T., "Development of Power Assisting Suit for Assisting Nurse Labor," JSME International Journal Series C, Vol. 45, No. 3, pp. 703-711, 2002.
3. Jeong, Y., Lee, D., Kim, K., and Park, J., "A Wearable Robotic Arm with High Force-Reflection Capability," Proceedings of the IEEE International Workshop on Robot and Human Interactive Communication, pp. 411-416, 2000.
4. Umetani, Y., Yamada, Y., Morizono, T., Yoshida, T., and Aoki, S., "Skil Mate, Wearable Exoskeleton Robot," IEEE International Conference on Systems, Man, and Cybernetics, Vol. 4, pp. 984-988, 1999.
5. Rosen, R. and Perry, J. C., "Upper Limb Powered Exoskeleton," International Journal of Humanoid Robotics, Vol. 4, No. 3, pp. 529-548, 2007.
6. Yagi, E., Harada, D., and Kobayashi, M., "Development of an Upper Limb Power Assist System Using Pneumatic Actuators for Farming Lift-up Motion," Journal of System Design and Dynamics, Vol. 3, No. 5, pp. 781-791, 2009.
7. Mehdi, H. and Boubaker, O., "Rehabilitation of a Human Arm Supported by a Robotic Manipulator: A Position/Force Cooperative Control," Journal of Computer Science, Vol. 6, No. 8, pp. 912-919, 2010.
8. Ding, M., Ueda, J., and Ogasawara, T., "Pinpointed Muscle Force Control Using a Power-assisting Device: System Configuration and Experiment," Proceedings of the 2nd IEEE RAS & EMBS International Conference on Biomedical Robotics and Biomechatronics, pp. 181-186, 2008.
9. Montagner, A., Frisoli, A., Marcheschi, S., Sanchez, E., and Bergamasco, M., "Optimal Control of a Robotic System for Human Power Enhancement," Proceedings of the 2nd Joint EuroHaptics Conference and Symposium on Haptic Interfaces for Virtual Environment and Teleoperator Systems, pp. 212-218, 2007.
10. Kazerooni, H., "Human-Robot Interaction via the Transfer of Power and Information Signals," IEEE Transactions on Systems, Man, and Cybernetics, Vol. 20, No. 2, pp. 450-463, 1990.
11. Kazerooni, H., Steger, R., and Huang, L., "Hybrid Control of the Berkeley Lower Extremity Exoskeleton (BLEEX)," The International Journal of Robotics Research, Vol. 25, No. 5-6, pp. 561-573, 2006.
12. Kawamoto, H., Kanbe, S., and Sankai, Y., "Power Assist Method for HAL-3 Estimating Operator's Intention Based on Motion Information," Proceedings of the 12th IEEE International Workshop on Robot and Human Interactive Communication, pp. 67-72, 2003.
13. Low, K. H., Liu, X., and Yu, H., "Development of NTU Wearable Exoskeleton System for Assistive Technologies," Proceedings of the IEEE International Conference on Mechatronics & Automation, Vol. 2, pp. 1099-1106, 2005.
14. Lee, H. D., Yu, S. N., Lee, S. H., Han, J. S., and Han, C. S., "Development of Human-Robot Interfacing Method for Assistive Wearable Robot of the Human Upper Extremities," SICE Annual Conference, pp. 1755-1760, 2008.
15. Bueno, L., Brunetti, F., Frizera, A., and Pons, J. L., "Human-Robot Cognitive Interaction, in: Pons, J. L. (Ed.), Wearable Robots: Biomechatronic Exoskeletons," John Wiley & Sons, pp. 87-125, 2008.
16. Rocon, E., Ruiz, A. F., Raya, R., Schiele, A., and Pons, J. L., "Human-Robot Physical Interaction, in: Pons, J. L. (Ed.), Wearable Robots: Biomechatronic Exoskeletons," John Wiley & Sons, pp. 127-163, 2008.
17. Abdullah, H. A., Tarry, C., Datta, R., Mittal, G. S., and Abderrahim, M., "Dynamic biomechanical model for assessing and monitoring robot-assisted upper-limb therapy," Journal of Rehabilitation Research & Development, Vol. 44, No. 1, pp. 43-62, 2007.
18. Adams, J. A., "Critical Considerations for Human-Robot

Interface Development," AAAI Fall Symposium on Human-Robot Interaction, pp. 1-8, 2002.

19. Size Korea, "Korea Human Scale," http://sizekorea.kats.go.kr/